


Fuzzy Proportional Integral Derivative control of a voice coil actuator system for adaptive deformable mirrors

Ziqiang Cui^{1,2,3}, Heng Zuo^{1,2*} , Weikang Qiao^{1,2,3}, Hao Li^{1,2}, Fujia Du^{1,2},
Yifan Wang^{1,2}, Jinrui Guo^{1,2,3}

¹Nanjing Institute of Astronomical Optics & Technology, Chinese Academy of Sciences, Nanjing 210042, China

²CAS Key Laboratory of Astronomical Optics & Technology, Nanjing Institute of Astronomical Optics & Technology, Nanjing 210042, China

³University of Chinese Academy of Sciences, Beijing 100049, China

*Correspondence: hengz@niaot.ac.cn

Received: February 29, 2024; Accepted: March 28, 2024; Published Online: April 20, 2024; <https://doi.org/10.61977/ati2024025>

© 2024 Editorial Office of Astronomical Techniques and Instruments, Yunnan Observatories, Chinese Academy of Sciences. This is an open access article under the CC BY 4.0 license (<http://creativecommons.org/licenses/by/4.0/>)

Citation: Cui, Z.Q., Zuo, H., Qiao, W. K., et al. 2024. Fuzzy Proportional Integral Derivative control of a voice coil actuator system for adaptive deformable mirrors. *Astronomical Techniques and Instruments*, 1(3): 179–186. <https://doi.org/10.61977/ati2024025>.

Abstract: Research on adaptive deformable mirror technology for voice coil actuators (VCAs) is an important trend in the development of large ground-based telescopes. A voice coil adaptive deformable mirror contains a large number of actuators, and there are problems with structural coupling and large temperature increases in their internal coils. Additionally, parameters of the traditional proportional integral derivative (PID) control cannot be adjusted in real-time to adapt to system changes. These problems can be addressed by introducing fuzzy control methods. A table lookup method is adopted to replace real-time calculations of the regular fuzzy controller during the control process, and a prototype platform has been established to verify the effectiveness and robustness of this process. Experimental tests compare the control performance of traditional and fuzzy proportional integral derivative (Fuzzy-PID) controllers, showing that, in system step response tests, the fuzzy control system reduces rise time by 20.25%, decreases overshoot by 78.24%, and shortens settling time by 67.59%. In disturbance rejection experiments, fuzzy control achieves a 46.09% reduction in the maximum deviation, indicating stronger robustness. The Fuzzy-PID controller, based on table lookup, outperforms the standard controller significantly, showing excellent potential for enhancing the dynamic performance and disturbance rejection capability of the voice coil motor actuator system.

Keywords: Adaptive optics; Deformable mirror; Voice coil actuator; Fuzzy control

1. INTRODUCTION

Adaptive optics (AO) is a dynamic wavefront correction technique^[1] with extensive applications in fields such as laser communication, ground-based optical telescopes, and imaging the retina of the human eye^[2]. As one of the key components of an adaptive optics system, deformable mirrors driven by piezoelectric materials are widely used and are a relatively mature technology, but they face challenges such as hysteresis, high driving voltage, and limited stroke. Deformable mirrors driven by VCAs are used in telescopes such as the Multiple Mirror Telescope (MMT)^[3], Large Binocular Telescope (LBT)^[4], and Very Large Telescope (VLT)^[5], owing to their advantages of fast response, no hysteresis, large stroke, and high precision. Internationally, upcoming next-generation large ground-based telescopes such as the Giant Magellan Tele-

scope (GMT) in the United States and the Extremely Large Telescope (ELT) in Europe are adopting this voice coil adaptive deformable mirror technology. Currently, there are no instances of the application of this technology in large telescopes within China.

Research on voice coil adaptive deformable mirrors is already underway in China^[6, 7], and the currently available literature primarily covers topics such as the structural design of voice coil motor actuators and the displacement detection of deformable mirror surfaces. However, there is a lack of relevant reports on the control algorithms employed in voice coil motor actuator systems. Currently, VCAs commonly employ PID control^[8, 9], with parameters that are often determined through empirical tuning, but this approach presents challenges such as sub-optimal correction effects and generally extended tuning times.

Voice coil adaptive deformable mirrors, which contain a large number of actuators, face challenges such as structural coupling between actuators and a significant temperature rise in the actuator coils. During the control process, the characteristics of the actuators can be affected, and PID control parameters are unable to dynamically self-tune to adapt to system changes in real-time. In response to the aforementioned issues, we propose a Fuzzy-PID control algorithm. This combined approach is then applied to the control of voice coil motor actuators, allowing real-time self-tuning of PID control parameters during the control process. Fuzzy control has the advantage of not relying on an accurate model of the controlled object, making it effective for controlling objects for which it is difficult to establish precise mathematical models^[10]. The Fuzzy-PID algorithm inherits the advantages of regular fuzzy control methods and also has the applicability and robustness of a PID control method. In addition, by employing a table lookup method instead of real-time calculations by the fuzzy controller, the computational complexity during the control process is reduced.

Here, we introduce the design of a Fuzzy-PID controller and the acquisition of a fuzzy control lookup table, and verify the effectiveness of the controller in improving the dynamic performance and disturbance resistance of voice coil motor actuators through both simulation and experimental approaches.

2. MATHEMATICAL MODELING OF A VOICE COIL MOTOR ACTUATOR

Adaptive deformable mirrors with numerous actuators face challenges in implementing centralized control methods and lack general design approaches for fully decentralized cooperative control^[11]. Here, we focus on the Fuzzy-PID control algorithm using a voice coil motor actuator from a self-developed six-unit voice coil adaptive deformable mirror. A schematic diagram of this is shown in Fig. 1.

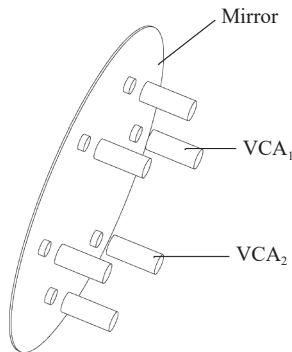


Fig. 1. Structure diagram for a voice coil actuator adaptive deformable mirror, VCA₁ and VCA₂.

The voice coil actuator system primarily consists of a deformable mirror, voice coil actuator, capacitive sensor, controller, driver, and base part. The voice coil actuator

used in this research is a counter-opposed voice coil actuator, where the rotor is a permanent magnet opposed to the coil. In this configuration, the coil is fixed to the base, and the rotor magnet is rigidly connected to the deformable mirror. The equivalent mechanical model and equivalent circuit diagram of the voice coil motor actuator are shown in Fig. 2.

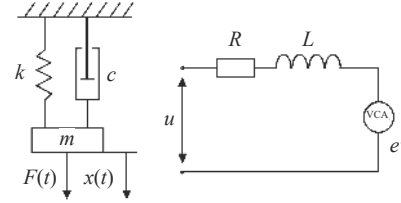


Fig. 2. The equivalent mechanical model and equivalent circuit diagram of the voice coil motor actuator.

According to Newton's laws of motion, the dynamic equilibrium equation for a voice coil motor actuator can be expressed as

$$m \frac{d^2x}{dt^2} + c \frac{dx}{dt} + kx = k_m i \quad (1)$$

and

$$F = k_m i, \quad (2)$$

where m is the total mass of the rotor, x is the displacement of the rotor, k is the spring elastic coefficient, c is the damping coefficient, i is the current in the coil, k_m is the motor force constant, and F is the electromagnetic force.

According to Kirchhoff's voltage law, the voltage equilibrium equation for the voice coil motor actuator can be expressed as

$$k_E \frac{dx}{dt} + L \frac{di}{dt} + iR = u \quad (3)$$

and

$$E_f = k_E \frac{dx}{dt}, \quad (4)$$

where k_E is the back electromotive force (EMF) coefficient, L is the equivalent inductance, R is the equivalent resistance, u is the coil terminal voltage, and E_f is the back EMF.

By combining equations (1) and (3), and performing Laplace transformation, the transfer function of the voice coil motor actuator can be obtained as

$$\frac{X(s)}{U(s)} = \frac{k_m}{mLs^3 + (cL + mR)s^2 + (LR + cR + k_m k_E)s + kR}. \quad (5)$$

Using the LabVIEW programming environment, a data acquisition program was developed to collect data using a uniform white noise signal (pseudo-random signal) as the input signal and the displacement of the voice coil motor actuator as the output signal. The input signal

frequency ranges are 0–120 Hz, 0–80 Hz, 0–50 Hz, and 0–40 Hz, with an amplitude of ± 0.5 V. Given that engineering typically focuses on the accuracy of identification models within the working bandwidth and considering that the resonance frequency of the six-unit voice coil motor deformable mirror is low, high-frequency noise signals may affect the results of system identification. Therefore, the data were preprocessed using the MATLAB system identification toolbox by filtering, mean removal, and resampling, then selecting “transfer function model” as the model type to be identified. Following the structure specified in equation (5) with 3 poles and 0 zeros, system identification is performed on the voice coil actuator. Multiple adjustments to the initialization methods are

made to select the optimal identification result. The resulting transfer function for the voice coil actuator is

$$\frac{X(s)}{U(s)} = \frac{1.026 \times 10^7}{s^3 + 519.2s^2 + 2.305 \times 10^5 s + 3.499 \times 10^7}. \quad (6)$$

3. FUZZY-PID CONTROLLER DESIGN

A Fuzzy-PID controller consists of both PID and fuzzy control components, as illustrated in Fig. 3. This arrangement takes error and the rate of change of error as inputs and adjusts PID parameters in real-time using fuzzy control rules.

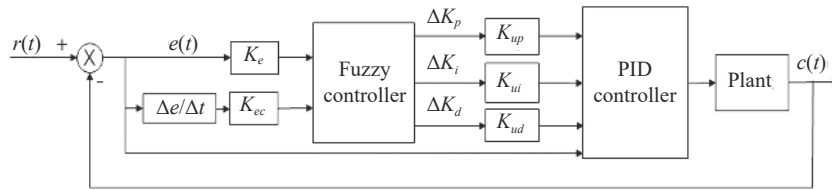


Fig. 3. Block diagram for a Fuzzy-PID controller.

Here, the chosen input variables for the fuzzy controller are the position deviation e and the rate of change of position deviation ec of the voice coil actuator. The output variables are the increments of the PID control parameters, Δk_p , Δk_i , and Δk_d , together with the corresponding fuzzy variables (linguistic variables) are E , EC , ΔK_p , ΔK_i , and ΔK_d . In Fig. 3, K_e and K_{ec} are quantification factors, and K_{up} , K_{ui} , K_{ud} are proportionality factors for the increments of the PID control parameters.

3.1. Input and Output Variables with Their Domains

Considering that this fuzzy control system is a multi-variable system with a large number of input and output variables, we adopted a standardized design. The fuzzy set domains of E , EC , Δk_p , Δk_i , and Δk_d are all set to $[-6, 6]$, and the linguistic values of fuzzy variables are NB, NM, NS, ZO, PS, PM, PB, where NB represents negative large, NM represents negative medium, NS represents negative small, ZO represents zero, PS represents positive small, PM represents positive medium, and PB represents positive large. Standardized design simplifies the complexity of fuzzy variable design, facilitates the understanding and formulation of fuzzy rules, and improves the universality of the control system, making it easy to extend the actuator control to other positions on the adaptive deformable mirror. Through multiple adjustments of quantification factors and proportionality factors in simulations, to optimize the controller performance, the domains for input and output variables are determined as $e = [-4, 4]$, $ec = [-30, 30]$, $\Delta k_p = [-1.2, 1.2]$, $\Delta k_i = [-4.8, 4.8]$, and $\Delta k_d = [-0.0006, 0.0006]$.

3.2. The Membership Functions and Fuzzy Rules

Fuzzy variables have multiple linguistic values, with

each linguistic value corresponding to a membership function. Common membership functions include triangular, Gaussian, and trapezoidal^[11]. In this study, the selection principle for membership functions is to use low-resolution fuzzy sets in regions with large errors and higher-resolution fuzzy sets in regions with smaller errors^[12]. Considering the practicalities, the adaptive deformable mirror has a high frequency but a small amplitude of motion. When the input deviation is small, there is a high requirement for control accuracy, while the accuracy requirement is relatively lower when the input deviation is large. Different membership functions have varied effects on control characteristics. For the portions where the central error is relatively small, functions with sharper shapes are employed. These functions are less influenced by other membership functions, resulting in higher control sensitivity. In contrast, for portions with larger errors, smoother-shaped functions are used, providing better stability performance. Considering both control sensitivity and stability, the membership functions for input and output linguistic variables are adjusted based on simulation experiments, as illustrated in Fig. 4. The linguistic value ZO adopts a triangular membership function; NM, NS, PS, PM use Gaussian membership functions; NB uses a Z-shaped membership function; and PB adopts an S-shaped membership function.

Fuzzy control rules have a direct impact on the performance of the fuzzy inference system. We comprehensively consider the control effectiveness of the three parameters k_p , k_i and k_d in the PID control algorithm, and the influence of the dynamic performance of the system when these three parameters change, such as the settling time and overshoot of the system's step response. Simultaneously, expert control experience is incorporated into the formulation of fuzzy rules. A fuzzy control rules table for

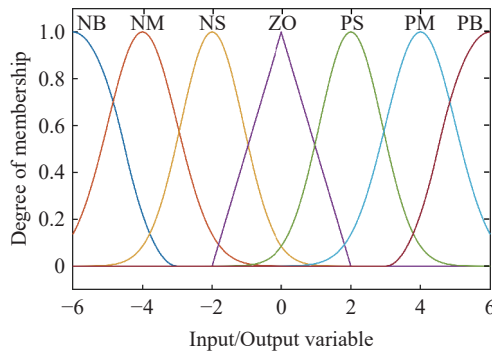


Fig. 4. Membership functions of input and output variables. The different linguistic values shown adopt different membership functions.

ΔK_P , ΔK_I , ΔK_D is formulated as shown in Table 1.

3.3. De-fuzzification

The Mamdani method^[13] is employed for fuzzy inference in this study, and the centroid method is used for de-fuzzification of fuzzy output. The centroid method assumes that the fuzzy set of fuzzy output is a two-dimensional plane, and the centroid of the plane is the weighted average of all points on that plane, with weights determined by the membership degrees of each point in the fuzzy set. These weights can be determined based on the membership functions and fuzzy rules obtained in subsection 2.2. Using the centroid method, precise outputs ΔK_P , ΔK_I and ΔK_D under the inputs e and ec are obtained.

The PID control parameters used in practical applications are obtained based on equation (7), where k_p , k_i , and k_d are the real-time PID control parameters; k_{p0} , k_{i0} and k_{d0} are the initial PID control parameters, and K_{up} , K_{ui} , K_{ud} are the proportion factors of PID control parameter increments determined through multiple simulation experiments. The proportion factors are multiplied by the

fuzzy controller outputs Δk_p , Δk_i , Δk_d to obtain real-time changes in PID control parameters. The relationship between these values can be mathematically expressed as

$$\begin{cases} k_p = k_{p0} + K_{up}\Delta k_p \\ k_i = k_{i0} + K_{ui}\Delta k_i \\ k_d = k_{d0} + K_{ud}\Delta k_d \end{cases} \quad (7)$$

These changes are then added to the initial PID control parameters to obtain real-time PID control parameters.

3.4. Retrieving the Fuzzy Control Lookup Table

With the development of voice coil adaptive deformable mirror technology, the number of voice coil motor actuators is increasing. Consequently, their control programs are becoming more complex, requiring high computational capabilities for the controllers. To reduce costs and decrease the computational load on the controller in real-time, this study adopts a table lookup method to replace the real-time calculation of the fuzzy controller. This means offline computation of a fuzzy control lookup table representing the relationship between input variables $K_e \cdot e$, $K_{ec} \cdot ec$ and output variables Δk_p , Δk_i , Δk_d . The compiled fuzzy control lookup table is then embedded in the controller. During on-site control, the software only needs to query the control table to obtain the required control quantities, which are then output to control the actual object^[14].

For ease of engineering implementation, in this paper, the range of variations for the input variables $K_e \cdot e$ and $K_{ec} \cdot ec$ is discretized into a set of 13 integers, specifically $\{-6, -5, -4, -3, -2, -1, 0, 1, 2, 3, 4, 5, 6\}$. The discretization method involves dividing the range of variations for $K_e \cdot e$ and $K_{ec} \cdot ec$ into 13 sub-intervals. Within each sub-interval, the values of $K_e \cdot e$ or $K_{ec} \cdot ec$ are assigned the same value. The assignment of values in different intervals is given in Table 2.

The MATLAB Fuzzy Logic Toolbox provides a graphi-

Table 1. Fuzzy rule table of ΔK_P , ΔK_I , ΔK_D

E	$\Delta K_P, \Delta K_I, \Delta K_D$						
	EC=NB	EC=NM	EC=NS	EC=ZO	EC=PS	EC=PM	EC=PB
NB	PB, NB, PS	PB, NB, NS	PM, NM, NB	PM, NM, NB	PS, NS, NB	ZO, ZO, NM	ZO, ZO, PS
NM	PB, NB, PS	PB, NB, NS	PM, NM, NB	PS, NS, NM	PS, NS, NM	ZO, ZO, NS	NS, ZO, ZO
NS	PM, NM, ZO	PM, NM, NS	PM, NS, NM	PS, NS, NM	ZO, ZO, NS	NS, PS, NS	NS, PS, ZO
ZO	PM, NM, ZO	PM, NM, NS	PS, NS, NS	ZO, ZO, NS	NS, PS, NS	NM, PM, NS	NM, PM, ZO
PS	PS, NM, ZO	PS, NS, ZO	ZO, ZO, ZO	NS, PS, ZO	NS, PS, ZO	NM, PM, ZO	PM, PB, ZO
PM	PS, NO, PB	ZO, ZO, NS	NS, PS, PS	NM, PS, PS	NM, PM, PS	NM, PB, PS	NB, PB, PB
PB	ZO, NO, PB	ZO, ZO, PM	NM, PS, PM	NM, PM, PM	NM, PM, PS	NB, PB, PS	NB, PB, PB

Table 2. Assignment of $K_e \cdot e$ or $K_{ec} \cdot ec$ in different intervals

Input	Interval												
	$(-\infty, -5.5)$	$[-5.5, -4.5)$	$[-4.5, -3.5)$	$[-3.5, -2.5)$	$[-2.5, -1.5)$	$[-1.5, -0.5)$	$[-0.5, 0.5)$	$[0.5, 1.5)$	$[1.5, 2.5)$	$[2.5, 3.5)$	$[3.5, 4.5)$	$[4.5, 5.5)$	$[5.5, +\infty)$
$K_e \cdot e$	-6	-5	-4	-3	-2	-1	0	1	2	3	4	5	6
$K_{ec} \cdot ec$	-6	-5	-4	-3	-2	-1	0	1	2	3	4	5	6

cal user interface. After completing the design of the fuzzy system using this interface, all combinations of discretized $K_e \cdot e$ and $K_{ec} \cdot ec$ are input, and the corresponding values of Δk_p , Δk_i , Δk_d are recorded. Subsequently, a fuzzy control lookup table can be obtained, representing

the relationship between the input variables $K_e \cdot e$, $K_{ec} \cdot ec$ and the output variables Δk_p , Δk_i , Δk_d [13]. Through the above process, we can obtain the fuzzy control lookup table for Δk_p as shown in Table 3. Similarly, lookup tables for Δk_i and Δk_d can be formulated.

Table 3. Fuzzy control query table of ΔK_p

$K_e \cdot e$	$K_{ec} \cdot ec$												
	-6	-5	-4	-3	-2	-1	0	1	2	3	4	5	6
-6	5.16	5.08	4.88	4.19	3.95	3.56	3.66	2.98	1.72	1.02	-0.121	-0.407	-0.411
-5	5.08	5.08	4.8	4.19	3.95	3.06	3.11	2.95	1.67	0.995	-0.297	-0.969	-0.987
-4	4.88	4.8	4.88	4.19	3.95	3.06	2.31	2.31	1.35	0.732	-0.286	-1.12	-1.57
-3	4.19	4.19	4.19	4.19	3.94	3.06	2.02	1.01	0.688	0	-0.732	-1.04	-1.66
-2	3.95	3.95	3.95	3.94	3.95	3.06	2.02	0.978	0	-0.688	-1.35	-1.67	-1.72
-1	3.92	3.91	3.67	3.06	3.06	2.12	0.994	-0.0132	-1.33	-2	-2.73	-2.94	-2.94
0	3.76	3.73	3.52	2.9	2.14	0.994	0.293	-0.794	-2.14	-2.9	-2.67	-2.69	-2.78
1	2.98	2.95	2.74	2	1.33	0	-0.794	-1.08	-2.4	-3.03	-1.26	0	0.102
2	1.72	1.67	1.35	0.688	0	-1.33	-2.14	-2.4	-2.31	-3.08	-1.75	0.278	2.42
3	1.66	1.04	0.732	0	-0.688	-2	-2.9	-3.03	-3.08	-3.08	-1.41	-0.551	0.152
4	1.57	1.11	0.00784	-1.27	-1.86	-2.74	-3.52	-3.67	-3.76	-3.72	-2.8	-3.17	-3.27
5	0.987	0.962	0.00812	-2.01	-2.83	-2.98	-3.73	-3.91	-3.93	-4.15	-4.2	-4.2	-4.59
6	0.411	0.399	-0.167	-2.04	-3.3	-3.53	-3.76	-3.92	-3.95	-4.19	-4.78	-4.69	-4.78

4. SIMULATION ANALYSIS

To compare the performance of the fuzzy and regular PID controllers, a simulation diagram was created in the MATLAB/Simulink environment, as shown in Fig. 5. The transfer function used in the simulation diagram is given by equation (6), with quantization factors $K_e = 1.5$ and $K_{ec} = 0.2$, and proportionality factors $K_{up} = 0.2$, $K_{ui} = 0.8$, $K_{ud} = 0.0001$.

By using a trial-and-error method and performing multi-

ple adjustments, the optimal initial parameters for the PID controller are selected as follows: $k_{p0} = 0.01$, $k_{i0} = 420$, $k_{d0} = 0.008$. In the simulation environment, a unit step signal is applied simultaneously to both control systems, with results shown in Fig. 6. According to Table 4, the fuzzy PID control system exhibits superior dynamic performance. Compared with the regular PID control system, the fuzzy PID controller has a 4.53% reduction in rise time, a 25.34% decrease in overshoot, and a 25.77% reduction in settling time.

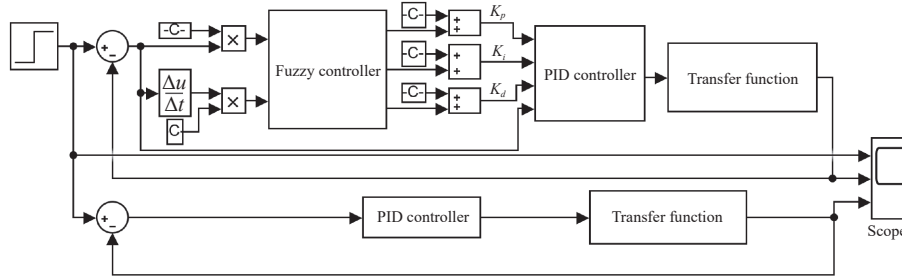


Fig. 5. Simulation block diagram of the fuzzy PID controller and PID controller. The upper section shows the construction of the fuzzy-PID control and the lower section shows a regular PID control.

Selecting another transfer function model obtained from system identification, for example equation (8), the fitting degree is lower compared to transfer function (6). By using transfer function (8), we conduct experiments again to compare the performance of PID controller and fuzzy PID controller. Per equation (8), gives a lower fitting degree compared with the transfer function (6). In the Simulink diagram above, without altering the controller parameters, the transfer function in the simulation diagram is replaced with equation (8) for simulation testing.

The results are shown in Fig. 7.

$$\frac{X(s)}{U(s)} = \frac{2.007 \times 10^7}{s^3 + 647.1s^2 + 3.681 \times 10^5 s + 7.67 \times 10^7} \quad (8)$$

As Table 5 shows, compared with the regular PID controller, although the rise time of the Fuzzy-PID controller increases by 0.92%, the overshoot decreases by 35.71%, and the settling time is shortened by 4.05%. When the transfer function of the voice coil motor actuator changes, the Fuzzy-PID controller demonstrates strong robustness,

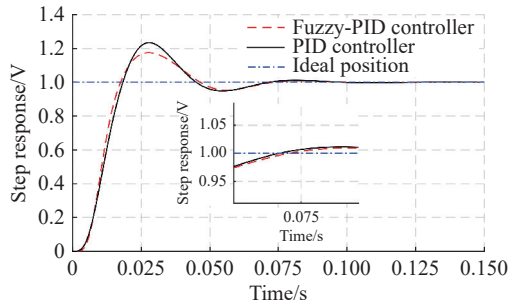


Fig. 6. Simulation step response curve showing different control methods.

Table 4. Performance comparison of transfer function (5) under different controllers

Controller	Raising time /ms	Overshoot /(%)	Settling time /ms
PID	18.32	23.44	56.51
Fuzzy-PID	17.49	17.50	41.95

Table 5. Performance comparison of transfer function (6) under different controllers

Controller	Raising time /ms	Overshoot /(%)	Settling time /ms
PID	19.51	12.60	38.98
Fuzzy-PID	19.69	8.10	37.40

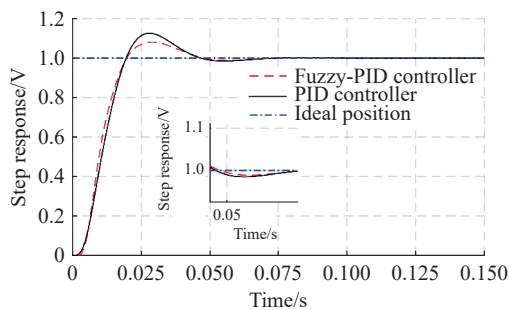


Fig. 7. Simulation step response curve after model change.

significantly improving the overshoot and settling time of the system response compared with a standard PID controller.

5. EXPERIMENTAL VERIFICATION

We created a prototype, shown in Fig. 8, using an NI cRIO-9040 embedded controller for both the Fuzzy-PID controller and the standard PID controller. This controller is equipped with a 16-channel 16-bit synchronous analog input module 9 220 with a measurement range of ± 10 V and a 16-channel 16-bit analog output module 9 264 with an output range of ± 10 V. We selected a capacitive sensor from MTI Instruments to collect displacement information from the voice coil actuator, with the sensor output ranging from 0–10 V and a range of 0–125 μm . Also employed here is a custom-built six-unit voice coil motor-driven adaptive deformable mirror, with the mirror surface facing down. The fuzzy control lookup table is com-

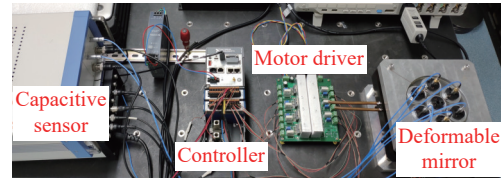


Fig. 8. Photograph showing the prototype control system.

piled into the controller, and a table lookup method is employed to replace the computations of the fuzzy controller. The PID controller uses a positional digital PID algorithm. At a control frequency of 1 kHz, the control effects of the PID controller and the Fuzzy-PID controller are tested and compared. At a control frequency of 1 kHz, the control effects of both types of controllers are tested and compared.

5.1. Comparison Experiment of Step Response Performance of Different Control Methods

VCA₁ (see Fig. 1) is initially set at 0 μm , while other actuators are in a constant-force maintenance state. The step response target position is 1 μm . The rise time and overshoot of the mirror reaching the target position are compared under different control methods. The response curves controlled by different methods are shown in Fig. 9. As shown in Table 6, the Fuzzy-PID control system exhibits improved dynamic performance. Compared with the regular PID control system, the Fuzzy-PID control has a rise time shortened by 20.25%, overshoot reduced by 78.24%, and settling time decreased by 67.59%.

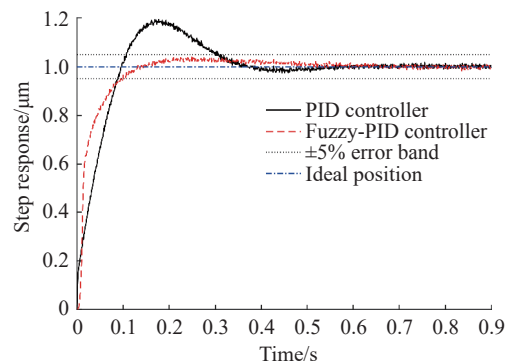


Fig. 9. Experimental curves of step responses for different control methods.

Table 6. Experimental results of control performance of different controllers

Controller	Raising time /ms	Overshoot /(%)	Settling time /ms
PID	79.00	19.39	307.00
Fuzzy- PID	63.00	4.22	99.50

5.2. Quantification and Proportionality Factor Impact Experiment

In the voice coil motor actuator system, to investigate the impact of quantization factors K_e and K_{ec} , as well

as the proportion factors K_{up} , K_{ui} , and K_{ud} (taking K_{up} as an example), on the performance of the Fuzzy-PID controller, experimental studies are conducted through a controlled variable method, with results shown in Fig. 10. The results indicate that within a certain range, K_e has a noticeable effect on reducing the rise time of the system, with a larger K_e resulting in a shorter rise time. K_{ec} has a significant effect on reducing the overshoot of the system, with a larger K_{ec} leading to a smaller overshoot. A larger K_{up} strengthens the corrective effect on PID control, effectively reducing the overshoot.

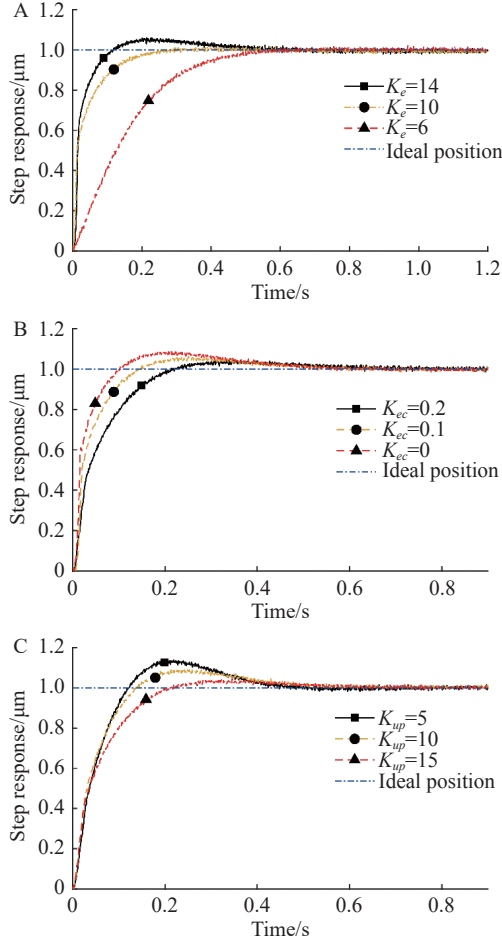


Fig. 10. The impact of parameters K_e , K_{ec} , and K_{up} on the results.

5.3. Anti-Disturbance Experiment

The steady-state position of VCA₁ is 1.25 μm . VCA₂ (as shown in Fig. 2) is selected to compare the robustness performance of the two controllers. A step command of 0.5 μm is applied to actuator VCA₂ on top of its current steady-state position of 1.25 μm . The displacement of the mirror at the position of voice coil motor actuator VCA₁ is recorded, and the experiment is conducted with 10 averaged results. The system responses under different controllers are compared, and the results, given in Fig. 11, indicate that the maximum deviation for PID is 69.30 nm, while for Fuzzy-PID, it is 37.36 nm. This demonstrates that, in the presence of a step disturbance from adja-

cent actuators, the maximum deviation is reduced by 46.09% with the Fuzzy-PID controller, as compared with the regular PID controller, showing improved robustness.

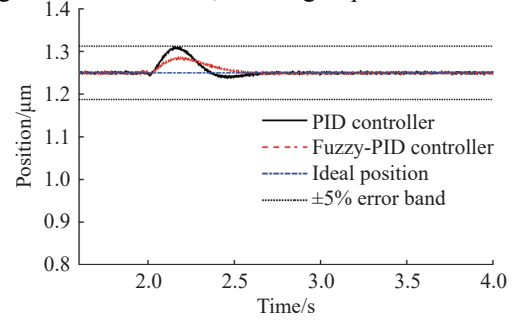


Fig. 11. Position fluctuation curve.

6. CONCLUSION

To address the issues of time-consuming adjustment of PID control parameters for voice coil motor actuators in adaptive deformable mirrors, as well as the inability to change parameters once they are determined, we propose the application of a Fuzzy-PID control algorithm. The fuzzy controller allows real-time self-tuning of PID control parameters. Considering the large number of voice coil motor actuators used in the adaptive deformable mirrors for large-aperture telescopes and the potential computational resource constraints faced by the controller hardware, our proposed system uses a table lookup method to replace the fuzzy controller calculations in actual control to save computational resources, as verified here by experimentation.

Our results show that, compared with standard PID control, Fuzzy-PID control reduces the rise time by 20.25%, decreases overshoot by 78.24%, and shortens the settling time by 67.59%. In disturbance rejection experiments, the maximum deviation under fuzzy control is reduced by 46.09% compared with standard PID control, showing stronger robustness. Additionally, we explore the influence of quantization factors and proportionality factors on the performance of the Fuzzy-PID controller.

In summary, the Fuzzy-PID control algorithm based on table lookup provides a reference for improving the dynamic performance and disturbance rejection capability of voice coil motor actuator systems for adaptive deformable mirrors. It also offers a method to mitigate the impact of changes in actuator system characteristic parameters, showing excellent potential for practical applications in future large telescopes.

ACKNOWLEDGEMENTS

This work is supported by the National Key R&D Program of China (2022YFA1603001, 2021YFC2801402), the National Nature Science Foundation of China (12073053), and the Science and Technology Plan of Inner Mongolia (2021GG0245).

AUTHOR CONTRIBUTIONS

Ziqiang Cui designed the Fuzzy-PID control algorithm and conducted experimental research. Weikang Qiao analyzed the experimental data and evaluated the effectiveness of the algorithm. Hao Li played a significant role in the construction of the experimental platform. Fujia Du validated the effectiveness of the experimental platform. Yifan Wang has improved some of the hardware of the experimental platform. Jinrui Guo organized the experimental results. Heng Zuo provided guidance for the experiment and proofread the manuscript, improving the overall quality of the manuscript. All authors have read and approved the final manuscript.

DECLARATION OF INTERESTS

Heng Zuo is an editorial board member for Astronomical Techniques and Instruments and was not involved in the editorial review or the decision to publish this article. The authors declare no competing interests.

REFERENCES

- [1] Guo, Y. M., Zhong, L. B., Min, L., et al. 2022. Adaptive optics based on machine learning: a review. *Opto-Electronic Advances*, **5**(7): 200082-1–200082-20.
- [2] Burns, S. A., Elsner, A. E., Sapoznik, K. A., et al. 2019. Adaptive optics imaging of the human retina. *Progress in Retinal and Eye Research*, **68**: 1–30.
- [3] Wildi, F. P., Brusa, G., Riccardi, A., et al. 2003. Towards first light of the 6.5m MMT adaptive optics system with deformable secondary mirror. In *Proceedings of SPIE*. 4839: 155–163.
- [4] Esposito, S., Riccardi, A., Fini, L., et al. 2010. First light AO (FLAO) system for LBT: final integration, acceptance test in Europe, and preliminary on-sky commissioning results. In *Proceedings of SPIE*. 7736: 107–118.
- [5] Arsenault, R., Biasi, R., Gallieni, D., et al. 2006. A deformable secondary mirror for the VLT. In *Proceedings of SPIE*. 6272: 284–295.
- [6] Zuo, H., Liu, Z. M. 2018. Design of microdisplacement measurement system for large aperture adaptive mirror. *Optics and Precision Engineering*, **26**(7): 1612–1620. (in Chinese)
- [7] Zhang, Z. G., Hu, Q. L., Ma, W. C., et al. 2022. Design and performance research of high efficiency variable reluctance voice coil actuator. *Chinese Journal of Liquid Crystal & Displays*, **37**(1): 21–28. (in Chinese)
- [8] Biasi, R., Gallieni, D., Mantegazza, P. 1996. Control law design for electromagnetic actuators at the secondary mirror. In *Adaptive Optics. ESO Conference and Workshop Proceedings*. 54: 221–227.
- [9] Deshmukh, P. G., Mandal, A., Parihar, P. S., et al. 2018. Design, development, and validation of a segment support actuator for the prototype segmented mirror telescope. *Journal of Astronomical Telescopes, Instruments, and Systems*, **4**(1): 014005.
- [10] Dai, J. K., Jiang, H. M., Zhong, Q. R., et al. 2014. LD temperature control system based on self-tuning fuzzy PID algorithm. *Infrared and Laser Engineering*, **43**(10): 3287–3291. (in Chinese)
- [11] Xu X., Li T., Bo, X., C., et al. 2000. *Matlab Toolbox Application Guide-Control Engineering*. Beijing: Publishing House of Electronics Industry. (in Chinese)
- [12] Wang, J. F., Lu, Z. D. 2000. The determine method of membership function in fuzzy control. *Henan Science*, **18**(4): 348–351.
- [13] Xi, A. M. 2008. *Fuzzy Control Technology*. Xi'an: Xidian University Press. (in Chinese)
- [14] Huangpu, H. Y., Zhang, X. Y. 2000. The design method of FUZZY controller-read table method and its application. *Journal of Xinjiang Normal University(Natural Sciences Edition)*, **19**(3): 29–33.